

IMAGE SEGMENTATION USING MULTILAYER COORDINATED CLUSTERS REPRESENTATION

Marcos J. Álvarez¹, Antonio Fernández¹, Elena González¹, Francesco Bianconi², Fernando J. Aguilar³ and Julia Armesto⁴

⁽¹⁾ *Universidade de Vigo*
ETSII, Departamento de Diseño en la Ingeniería
Vigo / Spain
E-mail: {marcos,antfdez,elena}@uvigo.es

⁽²⁾ *Università degli Studi di Perugia*
Dipartimento Ingegneria Industriale
Perugia / Italy
E-mail: bianco@unipg.it

⁽³⁾ *Universidad de Almería*
Escuela Politécnica Superior, Departamento de Ingeniería Rural
Almería / Spain
E-mail: faguilar@ual.es

⁽⁴⁾ *Universidade de Vigo*
ETSIM, Departamento de Ingeniería de Recursos Naturales y Medio Ambiente
Vigo / Spain
E-mail: julia@uvigo.es

Abstract

In this paper we present the rotation-invariant multilayer Coordinated Clusters Representation (CCR) colour texture descriptor. The central idea is to describe the colour content of an image by means of a reduced set of representative colours, and then to split the image into a stack of binary images, one for each colour of the reduced palette. The feature vector for each pixel consists of the codes of the correspond-

ing patterns of binary texture that occur in each layer. The validity of the model has been demonstrated through the segmentation of both synthetic mosaics of OuTex textures and multispectral IKONOS-2 satellite images. Experimental results show that the proposed features have high discriminative power and yield increased accuracy compared to other segmentation methods.

Keywords: *colour texture, image segmentation, CCR*

1 Introduction

Eyesight is the most important and complex human sense. It provides a great amount of sensorial information that is processed by the brain and let us interact with the world around. This fact justifies the significance of computer vision –image analysis using computers– as a research field. Recent advances in imaging devices and computer processing power have made feasible a wide variety of computer vision applications, such as remote sensing, medical diagnosis, robot vision, process monitoring, quality control or security, to cite some.

Image segmentation –splitting an image into meaningful regions of homogeneous properties– is a pre-processing stage in many computer vision applications. For image segmentation to be effective, a

proper characterization of the input image is needed. Unfortunately, there does not exist a general purpose, universal approach to feature extraction, and therefore, the feature set depends on the nature of and the information conveyed by the images to be processed.

Texture and colour are two of the most commonly used cues for image segmentation. These attributes have been traditionally regarded as separated phenomena. However, in recent years, fusion of colour and texture into a single model has received a great deal of attention [3, 4, 5, 6, 7, 9, 10, 13, 14, 18, 19, 20, 22].

Texture analysis techniques can be classified into four groups: *statistical, geometrical, model based* and *signal processing* methods [21]. The *Coordinated Clus-*

ters Representation (CCR) is a binary texture descriptor [11] that is halfway between geometrical and statistical methods. In this model a binary image is described by a histogram of occurrence of elementary patterns of binary texture –called *texels*– which are defined over a square window. The set of all the possible texels constitute a dictionary, in which each pattern is represented by a decimal code. For this method to be applied to grayscale images, a prior global binarization is required. This is a major issue, since the use of an inappropriate threshold can wipe out textural information.

Recently, a robust CCR-based model has been proposed for colour texture classification [5]. These features, known as rotation-invariant multilayer CCR, yield a twofold improvement with respect to the grayscale CCR model. First, this approach relies on circular rather than squared texels, which make the model insensitive against changes in texture orientation. Secondly, the new texture model benefits from colour information and makes it unnecessary to per-

form global thresholding.

In this paper we propose the application of rotation-invariant multilayer CCR to image segmentation. The central idea is to describe the textural and colour content of an image by splitting the original colour image into a stack of binary images. To evaluate the performance of the proposed features we have applied this method to the segmentation of different colour and multispectral images. Experimental results show that rotation invariant multilayer CCR features have a high discriminative power and yield increased accuracy with respect to other segmentation methods.

The remainder of this paper is organized as follows. In Section 2 we present the rotation-invariant multilayer CCR model for colour texture. Section 3 outlines the overall segmentation method. Section 4 details the benchmark data used in this article. Section 5 is devoted to describe the experimental results, and Section 6 summarizes the conclusions that can be drawn from this work.

2 Colour texture model

2.1 CCR features

The Coordinated Clusters Representation (CCR) is a binary texture descriptor [12]. In this model the feature vector is the histogram of occurrence of the possible binary patterns (texels) that can be defined over a square window. The dimension of these elementary patterns are usually set to 3×3 pixels, since this size provides good discriminative power at a reasonable cost in terms of both computing speed and memory consumption. In this case, the feature vector –denoted by $CCR_{3 \times 3}$ – has $2^9 = 512$ components. This binary texture descriptor was later extended to grayscale texture images through thresholding [11]. However, the need for global binarization is a major issue, since this preprocessing stage can wipe out textural information.

2.2 Rotation-invariant CCR

Another serious drawback of the CCR model is the sensitivity to changes in texture orientation, as even a small rotation can dramatically degrade performance. In practical applications it is of great importance that features be invariant against rotation, since images are rarely captured under steady viewing conditions. Rotation invariant CCR features can be obtained following an approach similar to the one proposed for the $LBP_{3 \times 3}$ operator [16].

The first step consists in replacing the squared neighbourhood used to compute the $CCR_{3 \times 3}$ by a circular neighbourhood. The intensity of the pixels that are not placed exactly on pixels positions is estimated

through bilinear interpolation. We denote this model by $CCR_{8,1}$.

In order to achieve rotation invariance, all the rotationally equivalent texels are mapped to the same pattern in the dictionary. This descriptor –denoted by $CCR_{8,1}^{ri}$ – reduces the dimension of the feature space from 512 to 72.

If we only consider the *uniform patterns*, i.e., those patterns where the number of transitions in the eight peripheral pixels is at most two, regardless of the value of the central pixel, a further reduction in the dimension of the feature space can be achieved. To be precise, there are 18 possible uniform texels in an 8-neighborhood of radius 1. The remaining non uniform patterns are accumulated into an additional 19th histogram bin. We refer to this feature space as the $CCR_{8,1}^{riu2}$.

2.3 Multilayer CCR

The multilayer CCR is an extension of the CCR that makes it possible to integrate texture and colour into a single model [5]. The central idea is to describe the colour content of an image by means of a reduced set of representative colours, and then to split the image into a stack of binary images, one for each colour of the reduced palette. To this end, each pixel is assigned an index encoding the colour of the palette which most closely resembles the pixel colour, and then is set to one in the layer corresponding to this index, and is set to zero in the remaining layers. The overall feature vector for each pixel is formed by the

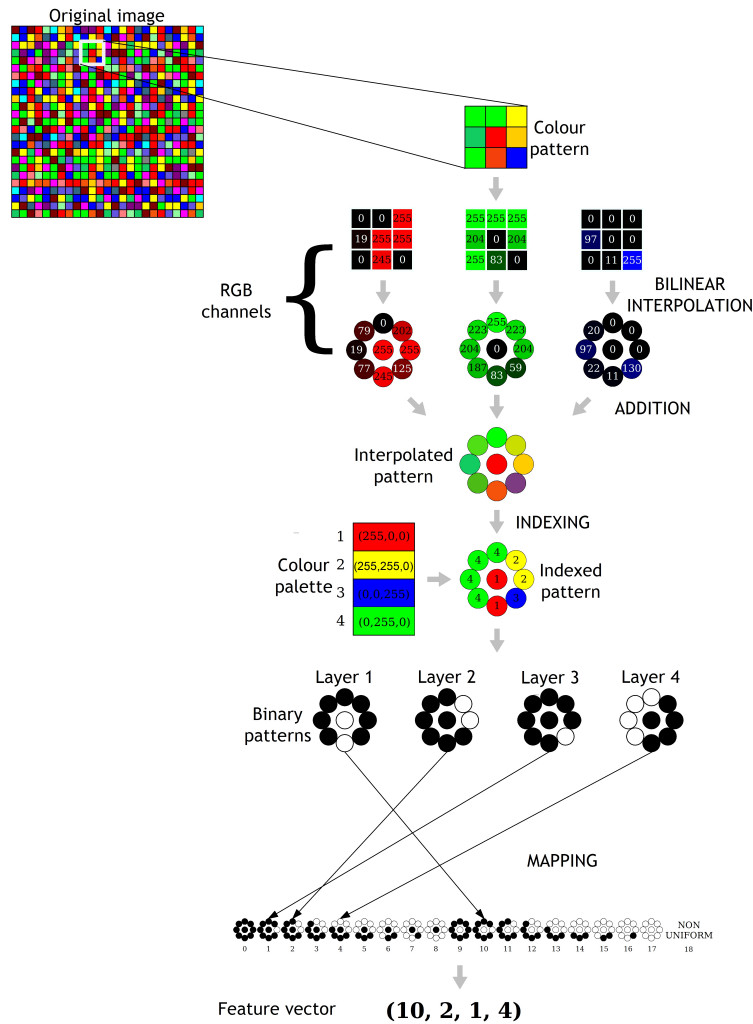


Figure 1: Schematic representation of the procedure to extract rotation-invariant multilayer CCR features

codes of the corresponding binary patterns that occur in each layer.

There are two main approaches to generate the reduced colour palette. On the one hand, a general purpose palette can be generated by *colour space quantization*, which can be straightforwardly implemented by dividing the RGB colour cube into equal-sized parallelepipeds. This implies that the resulting palette is fixed and it is the same for all the images to be processed. This approach has been successfully applied to colour texture classification [5]. Colour space quantization can be readily generalized to multispectral imaging by partitioning the n -dimensional space into equal-sized buckets. On the other hand, a data-dependent palette can be generated through *colour clustering*. In doing so, the palettes corresponding to different input images are themselves different since

the resulting palette contains the most representative colours of the image to be processed. We tested both approaches and found that colour clustering significantly outperforms uniform colour space quantization. Based on the results of this preliminary study we adopted the latter approach, using one of the most popular colour clustering implementations: the k -means algorithm.

Once the colour palette is generated, the colour triplet—or n -tuple in case of multispectral imaging—of each pixel is replaced by the index of the colour in the palette that most closely resembles the original colour. This process is referred to as *colour indexing*. To that end, it is necessary to quantitatively define the “closeness” of a pair of colours. Several similarity measures have been proposed in the literature. In this work we used the euclidean distance.

3 Description of the method

The segmentation process is divided into two clearly differentiated stages: training and testing. The first step of the training phase consists in generating a reduced colour palette of representative colours, through either uniform colour space quantization or colour clustering, as discussed in Section 2.3. We found that colour clustering outperforms uniform colour space quantization in roughly 20 percentage points of segmentation accuracy, and hence this was the approach we adopted. In our implementation the n -tuples of the original image were fed to the k -means clustering algorithm, where n denotes the number of bands of the image. Then, the 3×3 square neighbourhoods are transformed into circular neighbourhoods through bilinear interpolation (see Section 2.2), and subsequently, each pixel is assigned the index of the closest colour in the palette. In this work we used the euclidean distance in the colour space as a similarity measure between two colours.

The next step lies in assigning a feature vector to each pixel. For this aim, the indexed circular patterns are split into N binary circular patterns, one binary pattern for each colour of the palette. A pixel that has been assigned the index i in the indexed pattern takes a value of 1 in the binary pattern corresponding to colour i , and 0 in the rest of the binary patterns. The resulting N circular binary patterns are mapped to their associated rotationally equivalent binary patterns, which are represented by a decimal code. The pixel is finally assigned a feature vector which is made up of the codes of the corresponding elementary patterns. The overall procedure is schematically de-

picted in Figure 1.

It is well known that the learning algorithm must match the structure of the domain. Since we had a limited knowledge beforehand, we considered that it would be worthy to try different classifiers in order to choose the best suited for our particular application. To accomplish this task we used the *Waikato Environment for Knowledge Analysis* (WEKA¹) workbench [23]. The error rates obtained in these trials were very similar, independently of the classification scheme. In view of this, we chose the RandomTree algorithm [23], due to its inherent ability to manage with the kind of features we propose in this paper and its reasonable computational complexity.

In the testing phase we have to compute rotation-invariant multilayer CCR features for each pixel of the image to be processed following the method just described, with the only difference that in this case we have to use the palette generated in the training phase. These features are then fed to the RandomTree classifier which was previously learned, and as a result the class membership of each pixel is determined. It is convenient to note that in order to make a realistic estimation of the generalization error, the image used for testing should be different from the image used for training.

Finally, to evaluate the accuracy of the method, segmentation results are shown as indexed maps, where the pixel labels assigned by the classification algorithm are colour-coded for visualization purposes. Besides these maps, we computed several figures of merit to quantitatively assess performance.

4 Benchmark data

In order to assess the validity of the proposed method, we applied the rotation invariant multilayer CCR model to the segmentation of two different types of images, which are briefly described in the following subsections.

4.1 Synthetic images

The first group of images is formed by synthetic mosaics of OuTex textures. OuTex is being increasingly used as an evaluation framework by the computer vision community [17]. We have chosen a subset of 25 textures of the group *inca 100dpi* from the OuTex library. Five different mosaics of 746×538 pixels have been generated, each mosaic being formed by five different textures, as shown in Figure 2. It is important to note that the mosaics used for training contain

the same textures than the mosaics used for testing, but as one can readily see from Figures 2(a) and 2(b), the patches of a given texture in the train mosaic and the test mosaic correspond to non overlapping samples of the original OuTex texture. The mosaics were created this way in order to keep the training and testing stages independent of each other, and hence, to avoid underestimation of the generalization error.

4.2 Satellite imagery

The second dataset is formed by high resolution IKONOS-2 satellite imagery –R, G, B and NIR bands– of an area in the east of the Almería province –south-eastern Spain–. Two non overlapping subimages of 498×465 pixels and 634×594 pixels have been cropped from the whole image, one for training and

¹<http://www.cs.waikato.ac.nz/ml/weka/>

one for testing. These images are shown in Figure 3(a). The goal is to detect the areas covered by greenhouses. Greenhouse agriculture located in the southeast of Spain concentrates the highest production of vegetables in the Iberian peninsula. The economic strength of this sector has caused a rapid and uncontrolled greenhouse surface expansion, and as a

consequence, environmental threats have arisen [1]. A proper way to measure and control the covered surface and its evolution through time is being increasingly demanded by the government. The application of remote sensing and image processing techniques would be a helpful tool for the agricultural authorities to manage the greenhouse sector.

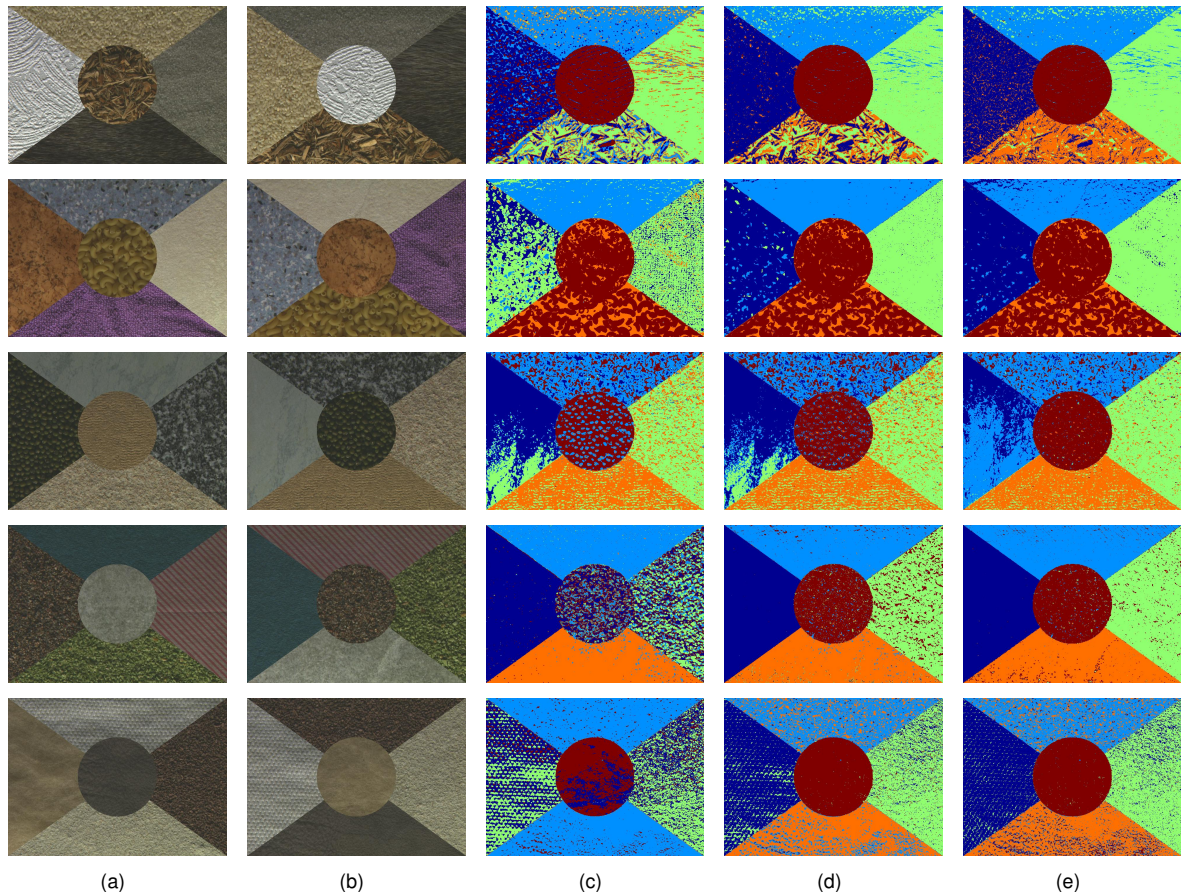


Figure 2: Synthetic mosaics of OuTex textures: (a) train images, and (b) test images, and segmentation results obtained using a palette of: (c) 5 colours, (d) 15 colours, and (e) 35 colours. Each row corresponds to a different mosaic.

5 Experimental results and discussion

We performed a set of segmentation experiments using the rotation invariant multilayer CCR over the two datasets described in the preceding section. We firstly studied the influence of colour quantization on the performance of the proposed approach. We found that segmentation accuracy is strongly affected by the number of colours that form the reduced colour palette. Figures 2(c) - 2(e) –corresponding to a palette of 5, 15 and 35 colours respectively– clearly show that the greater the palette size, the higher the segmentation accuracy, as one could expect. However, it should be noted that enlarging the colour

palette beyond a certain limit is impractical, since it would dramatically increase the computational burden. In addition to the visual assessment provided by Figure 2, we computed the percentage of pixels correctly classified as a figure of merit for the segmentation. Quantitative results obtained for OuTex mosaics are gathered in Table 1. One can easily notice from both this table and Figures 2(c) - 2(e) that there is a great spread in performance: a success rate close to 100% can be achieved, but there are also cases in which considerable confusion between classes occur. This fact is most evident in coarse textures and when

a mosaic contains two or more patches with similar visual appearance.

The second part of the experimental activity focuses on the satellite imagery described in Section 4.2. Herein the objective is to discriminate the greenhouses from the rest of elements in the image –soil, roads, water pools, etc.–. By simply viewing Figure 3(a) one can see that not all the greenhouses have the same appearance. These differences should not be surprising, as it is well-known that the spectral signature of plastic changes drastically with the angle of vision, its chemical composition and even its age [2]. It is fair to think that considering all the greenhouses as belonging to a unique class would lead to under-detection. Thus, we have grouped the greenhouses into four types from mere visual inspection. Figure 3(b) shows the manually defined ground truth, and Figure 3(c) shows the segmentation results. Careful observation of the lower rightmost corner of region A reveals the presence of abandoned greenhouses, which will likely introduce classification errors. Apart from the percentage of pixels correctly classified, we computed two additional figures of merit: *sensitivity* and *precision*. Sensitivity measures the proportion of target pixels correctly classified. Precision is the number of true positives divided by the total number of elements labelled as positives, so it can be regarded as a measure of exactitude [23]. The numerical results are gathered in Table 2. It should be noted that in the calculation of these figures of merit only two classes are considered: ‘greenhouse’ and ‘background’, and therefore, all the pixels labelled as greenhouse –irrespective of the particular type of greenhouse– are merged into a single class. In this experiment, the palette size was set to 15, since this number of colours gives a good balance between segmentation accuracy and computational

cost. Although IKONOS-2 imagery consists of 4 bands (R, G, B and NIR), we have used only the RGB bands because we found that considering the infrared band provides a negligible improvement on accuracy, at the price of significantly increasing the computational burden.

The performance of the proposed features was compared with two different approaches. First, we considered the well-known *Bayesian classifier* [8], a technique commonly used in many classical pattern recognition problems. We have also considered a state-of-the-art algorithm, the *Spatial AdaBoost* [15], an improvement over original AdaBoost which –for each pixel– takes into account contextual information of the neighbourhood. In both approaches the feature vector for each pixel is directly given by the band intensities: a RGB triplet in OuTex mosaics and a RGB/NIR 4-tuple in IKONOS-2 imagery. The results of these tests are shown in Figures 4(a) and 4(b), and Table 3.

A brief analysis of Figure 3(c) allows one to realize that the vast majority of incorrectly classified pixels either are isolated pixels or belong to small speckles, giving a noisy aspect to the results. This could be so because the segmentation algorithm works on a per-pixel basis, i.e., each pixel is assigned a class label based exclusively on its feature vector. As described in Section 2.3, this feature vector only takes into account a 3×3 pixel neighbourhood, disregarding the spatial relationships with more distant pixels. One could reasonably expect that removing the small isolated clusters of wrongly classified pixels from the segmented image would increase accuracy. To this end we successfully implemented diverse morphology and smoothing filters, which gave rise to improved outcomes, as can be ascertained from Figure 4(c) and Table 3.

6 Conclusions

In this paper we presented the rotation invariant multi-layer CCR descriptor for colour texture. The validity of the proposed model has been demonstrated through the segmentation of both synthetic mosaics and satellite imagery. Experiments show that the proposed colour texture features have high discriminative power and yield increased accuracy compared to other seg-

mentation methods, such as the maximum a posteriori probability rule and Spatial AdaBoost. Furthermore, the proposed feature set is robust, since similar segmentation results are obtained by employing different classifiers. These findings encourage further research to solve some open issues, such as optimal palette generation and class separability.

References

- [1] F. Agüera, F. J. Aguilar, and M. A. Aguilar. Using texture analysis to improve per-pixel classification of very high resolution images for mapping plastic greenhouses. *ISPRS Journal of Photogrammetry and Remote Sensing*, 63:635–646, 2008.
- [2] F. Agüera, M. A. Aguilar, and F. J. Aguilar. Detecting greenhouse changes from QuickBird imagery on the mediterranean coast. *International Journal of Remote Sensing*, 27:4751–4767, 2006.

Table 1: Percentage of pixels correctly classified in OuTex mosaics. The mosaic number refers to the corresponding row in Figure 2

Mosaic	Number of colours		
	5	15	35
1	70.58	83.73	89.90
2	62.94	80.82	80.16
3	74.40	75.64	77.64
4	75.23	93.84	96.92
5	53.74	84.38	85.20

Table 2: Numerical results (expressed in percentage) obtained for IKONOS-2 satellite imagery

Test area	Success rate	Sensitivity	Precision
A	86.68	65.71	84.06
B	82.38	81.01	69.53

- [3] M. A. Akhloufi, W. B. Larbi, and X. Maldague. Framework for color-texture classification in machine vision inspection of industrial products. *IEEE International Conference on Systems, Man and Cybernetics*, pages 1067–1071, 2007.
- [4] V. Arvis, C. Debain, M. Berducat, and A. Benassi. Generalization of the cooccurrence matrix for colour images: application to colour texture classification. *Image Analysis and Stereology*, 23:63–72, 2004.
- [5] F. Bianconi, A. Fernández, E. González, D. Caride, and A. Calviño. Rotation-invariant colour texture classification through multilayer CCR. *Pattern Recognition Letters*. Submitted in 2008.
- [6] F. Bianconi, A. Fernández, E. González, and F. Ribas. Texture classification through combination of sequential colour texture classifiers. *Lecture Notes in Computer Science*, 4756:235–243, 2007.
- [7] A. Drimbarean and P.F. Whelan. Experiments in colour texture analysis. *Pattern Recognition Letters*, 22:1161–1167, 2001.
- [8] R. C. González and R. E. Woods. *Digital Image Processing*. Pearson Prentice Hall, 2008.
- [9] D. Iakovidis, D. Maroulis, and S. Karkanis. A comparative study of color-texture image features. *Proceedings of the IEEE International Workshop on Systems, Signal and Image Processing (IWSSIP)*, pages 205–209, 2005.
- [10] A. Khotanzad and J. Bennett. A classification methodology for color textures using multispectral random field mathematical models. *Mathematical and Computational Applications*, 11:111–120, 2006.
- [11] E. V. Kurmyshev, R. E. Sánchez-Yáñez, and F. J. Cuevas. A framework for texture classification using the coordinated clusters representation. *Pattern Recognition Letters*, 24(1-3):21–31, 2003.
- [12] E.V. Kurmyshev and M. Cervantes. A quasi-statistical approach to digital binary image representation. *Revista Mexicana de Física*, 42:104–116, 1996.

Table 3: Percentage of correctly classified pixels for different segmentation methods

Test image	Bayes	Spatial AdaBoost	Our approach	
			without filtering	with filtering
Figure 2(b) , first row	85.52	89.73	89.90	99.79
Figure 3(a)	85.28	75.35	86.68	96.45

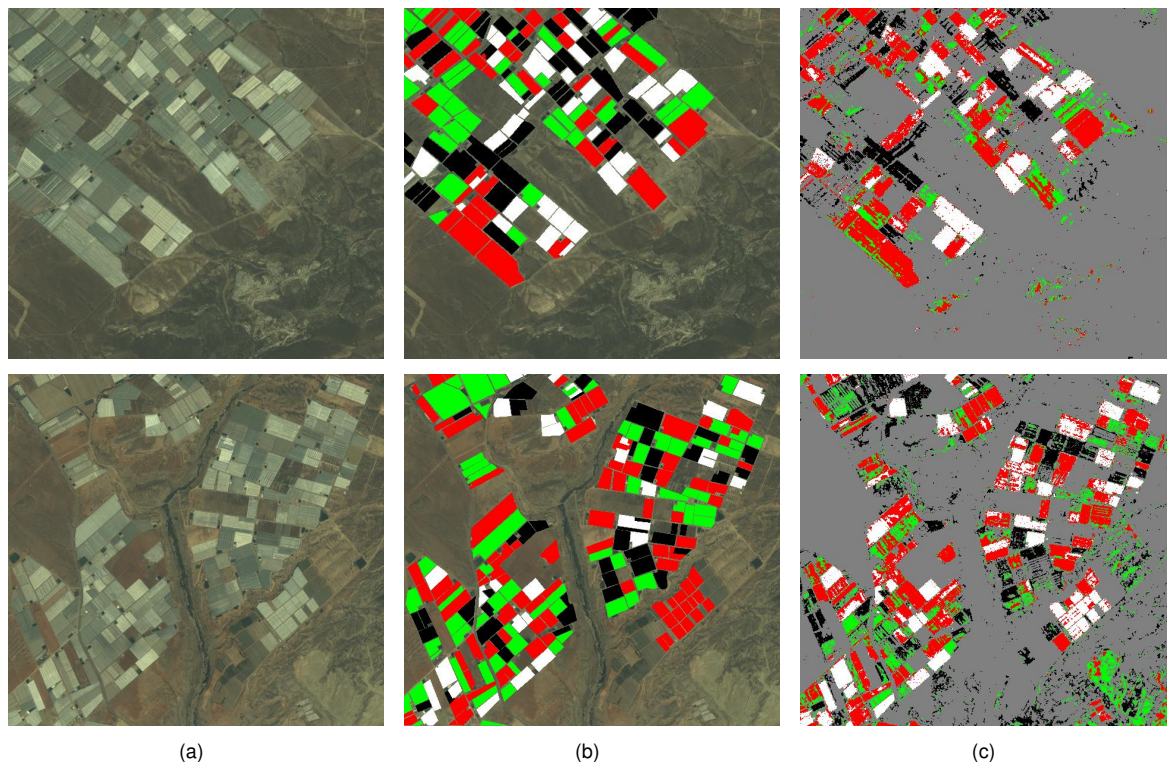


Figure 3: (a) IKONOS-2 images, (b) ground truth, and (c) detected greenhouses. First row correspond to region A, and second row correspond to region B.

- [13] T. Mäenpää and M. Pietikäinen. Classification with color and texture: jointly or separately? *Pattern Recognition*, 37:1629–1640, 2004.
- [14] M. Mirmehdi and M. Petrou. Segmentation of color textures. *IEEE Transactions on Pattern Analysis and Machine Intelligence*, 22:142–159, 2000.
- [15] R. Nishii and S. Eguchi. Robust supervised image classifiers by spatial AdaBoost based on robust loss functions. In *Proceedings of SPIE*, volume 5982, page 59820D, 2005.
- [16] T. Ojala, M. Pietikäinen, and T. Mäenpää. Multiresolution gray-scale and rotation invariant texture classification with Local Binary Patterns. *IEEE Transactions on Pattern Analysis and Machine Intelligence*, 24:971–987, 2002.
- [17] T. Ojala, M. Pietikäinen, T. Mäenpää, J. Viertola, J. Kyllönen, and S. Huovinen. Outex - new framework for empirical evaluation of texture analysis algorithms. In *Proceedings of the 16th International Conference on Pattern Recognition*, pages 701–706, 2002.
- [18] C. Palm. Color texture classification by integrative co-occurrence matrices. *Pattern Recognition*, 37:965–976, 2004.
- [19] K.Y. Song, J. Kittler, and M. Petrou. Defect detection in random colour texture. *Image Vision and Computing*, 14:667–683, 1996.
- [20] T.S.C. Tan and J. Kittler. Colour texture analysis using colour histogram. *Proceedings: Vision, Image and Signal Processing*, 141:403–412, 1994.
- [21] M. Tuceryan and A. K. Jain. Texture analysis. In *The Handbook of Pattern Recognition and Computer Vision (2nd Edition)*, pages 207–248, River Edge, NJ, USA, 1998. World Scientific Publishing Co., Inc.
- [22] G. Van de Wouwer, P. Scheunders, S. Livens, and D. Van Dyck. Wavelet correlation signatures for color texture characterization. *Pattern Recognition*, 32:443–451, 1999.
- [23] I. H. Witten and E. Frank. *Data Mining: Practical Machine Learning Tools and Techniques*. Morgan Kaufmann Series in Data Management Systems. Morgan Kaufmann, second edition, June 2005.

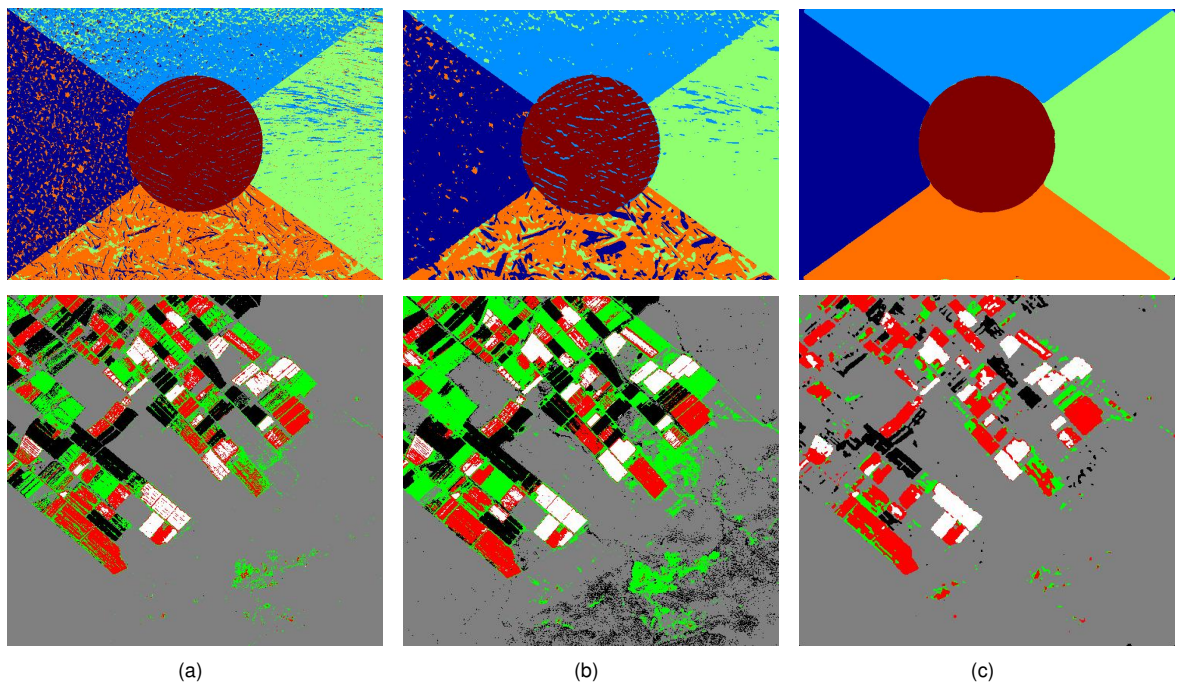


Figure 4: Segmentation results obtained using: (a) Bayesian classifier, (b) Spatial AdaBoost, and (c) rotation-invariant multilayer CCR, RandomTree classifier and median filtering. The test images corresponding to the first and second rows are Figure 2(b) (second row) and Figure 3(a), respectively.